RESEARCH ARTICLE

Photocatalytic Degradation of Methyl Orange Using Iron Oxide Nanoparticles Using Lotus Seeds

Renuka Subramaniam*, Nadachi Kumarasami , Vinothkumar Natarajan, Kowsalya Nagarajan, Dayanithi Mahalingam , Nirmal Damodaran , Anandhababu Manikkam, Krishna Kumar Sanniyasi

Department of Chemical Engineering,
Mahendra Engineering College (Autonomous),
Mallasamudram, Namakkal, TamilNadu-637503, India

ABSTRACT: In this study, the iron oxide nanoparticles were synthesised by green synthesis technique using lotus seed extract. The phytoconstituents present in the seed extract play a significant role in the fabrication of nanoparticles and acts as a stabilizing, reducing and capping agent. The prepared iron oxide nanoparticles were analysed using various techniques such as X–ray diffraction (XRD), scanning electron microscope (SEM), Fourier transformed infrared spectroscopy (FT-IR), Energy dispersive X–ray, and UV–Visible spectroscopy techniques. XRD result reveals that the average crystallite size was 45.1 nm and the crystallite shape was face – centred cubic in structure. The band gap energy of α-Fe_2O_3 nanoparticles was calculated to be 2.74 eV from UV–Visible analysis. The dye was determined using iron oxide nanoparticles. The photocatalytic degradation efficiency of methyl orange was achieved about 93.5 % in the conditions of 50 ml of 100 mg/L dye concentration, pH = 7.0, 10 mg/ml α-Fe_2O_3 and reaction time 120 minutes. The results of this study highlights that the nanomaterials prepared through green route have great importance in dye degradation applications.

KEYWORDS: Green synthesis, Lotus seed extract, Iron oxide nanoparticles, Methyl orange, Photocatalysis

https://doi.org/10.29294/IJASE.11.1.2024.3867-3874

1. INTRODUCTION

Water pollution is getting increased day by day due to the discharge of toxic and non-degradable compounds in recent years [1,2]. There are about 10,000 dyes that are manufactured and being used for different applications. The removal of dye compounds from waste water is a great challenge because of its high water solubility, chemical, photo and thermal stability. The release of untreated waste water with the presence of dyes can cause adverse health effects to the humans and surrounding environment. Methyl orange (MO) is one of the commonly used dyes in textile industries for colouring fibers, cotton, silk and wool. Moreover, a long exposure to MO may cause serious issues such as skin irritation, respiratory problems and mental disorders [3,4]. Therefore, an efficient material is urgently required to degrade successfully various dye pollutants.

Iron based transition metal oxides are widely exploited for photocatalytic degradation of dyes due to its different metal-oxygen ratios, narrow band gap, stable thermodynamic phase and varied structure–activity relationship properties. α-Fe_2O_3 is one of the most commonly utilized polymorph in photocatalytic degradation of dyes due to its exceptional electronic, high corrosion resistance, chemical stability, and mechanical properties. But the major drawback of this photocatalyst is its high recombination rate of photogenerated electrons and holes (<10 ps) [5, 6]. There are several methodologies such as hydrothermal, co-precipitation, sol-gel, solvothermal, electrochemical and chemical precipitation are followed to prepare iron oxide nanoparticles with low photogenerated charge carrier recombination rate [7-10]. The major drawbacks in hydrothermal process are limited scalability and specialized equipments requirement to maintain the preparation conditions. In the electrochemical method, the limitations are one can use only materials that is

**Corresponding Author: rsshekeena89@gmail.com*
Received: 20.07.2024 **Accepted:** 20.08.2024 **Published on**: 27.09.2024

having the property to be deposited electrochemically. In co-precipitation method, controlling the particle size and distribution is difficult, which requires careful control of pH and temperature. Therefore, a lot of attention has gained recently to fabricate iron oxide nanomaterials (α-Fe_2O_3 NPs) using plant extracts to reduce the charge carriers recombination rate. The idea of undertaking green route is to avoid the use of toxic chemicals and high energy requiring procedures. Moreover, the plant extracts included into the preparation of nanomaterials has the ability to increase the photoactivity of the metal oxides [11-13]. Because of the synergistic effect, the light absorption ability, electron-hole pairs separation, and the photocatalytic efficiency of obviously could be improved.

Hence, the present work mainly focuses on the biosynthesis of iron oxide nanoparticles by employing lotus seed extract, as a reducing and capping agent and also to investigate the ability of the material for the photocatalytic degradation of methyl orange dye.

2. MATERIALS

Iron chloride ($FeCl_3$) was obtained from Mercury scientific chemicals, Salem, Tamil Nadu. Lotus seeds were gathered from local surrounding in Salem district. Methyl orange dye (MO), distilled water, Whatman filter paper (Grade No. 1), and ethanol was purchased from Chemico glass and scientific company, Erode, Tamil Nadu.

2.1. Preparation of lotus seed extract

The lotus seeds were washed in distilled water. After cleaning, the seeds were allowed to dry. The dried seeds were grounded into powder consistency. 20 g of lotus seeds powder were added to 100 ml of distilled water and continuous stirring for 1 hour at 60X on a hot plate. After one hour the solution was allowed to reach the room temperature. Using Whatman filter paper the extract was filtered and kept the extract for further use at 4°C.

2.2. Synthesis of iron oxide nanoparticles

1 gm of ferric chloride was mixed with 10 ml of lotus seed extract. Then, the solution was stirred for 1 hour at 25°C. The colour change is occurred as a result of iron oxide nanoparticles produced. Later, the obtained solution was centrifuged twice for 15 mins at 4000 rpm. Then, the particles were washed with ethanol and water alternatively for three times. Finally, the sample was dried for two hours at 60 ºC in hot air oven.

2.3. Characterization of iron oxide nanoparticles:

The synthesized iron oxide nanoparticles (α-Fe_2O_3 NPs), were analysed through different techniques such as SEM-EDX, XRD, FTIR and UV–Visible spectroscopy. The scanning electron microscopy technique (SEM, JEOL (JEM-2100F), 100 kV) was used for the morphology analysis of iron oxide nanoparticles. X – ray diffraction (XRD), Cu – Kα radiation at a wavelength of 1.541 nm, 2θ at 20°- 80° was used to detect the structural properties and phase identification of iron oxide nanoparticles through Bruker D8 advanced powder diffractometer. A Fourier transform infrared microscopy (Spectrum 65 FTIR, Perkin Elmer) was used to study the morphological characteristics and O-H bonding of iron oxide nanoparticles from 4000-400 cm^{-1} wavelength range. A UV–Vis spectrometer (Philips 8800) was used to study the photocatalytic reaction. The optical band gap of sample powders was studied using $BaSO_4$ as reference sample from 310 to 800 nm to record the absorption peaks of iron oxide nanoparticles.

The photocatalytic activity of iron oxide nanoparticles was investigated using 50 mL of 10 ppm MO dye and 10 mg of catalyst was added in a round bottom flask under stirring condition at dark room. The flask containing the reaction mixture was placed 15 cm away the lamp source. Then, the solution was irradiated to light (250 W Halogen, Philips, India). Afterwards, 2 mL of sample were withdrawn at specific time intervals and absorbance was measured by UV–Vis spectrometry. MO concentrations were measured without using light irradiation and iron oxide nanoparticles.

3. RESULT AND DISCUSSION

3.1. X – ray diffractometer (XRD) analysis of Fe_2O_3 NPs

The crystalline properties of green synthesised iron oxide nanoparticles have been examined by XRD analysis as shown in Figure.1. The XRD patterns of iron oxide nanoparticles (α-Fe_2O_3 NPs) showed distinctive peaks at 2θ values of

29.72°, 35.62°, 38.83°, 49.08°, 61.80° and 66.46° corresponding to (012), (104), (110), (024), (214) and (300), respectively. The XRD pattern confirmed that no other impurity peaks were found. The XRD pattern was agreed well with the usual α-Fe_2O_3 peaks. Further, no other Fe_2O_3 polymorph was seen in the XRD result of the sample. Further, the crystallite size of iron oxide nanoparticles was determined by using Debye Scherrer's formula.

$$D = k\lambda / \beta \cos\theta$$

In the above equation, D refers the crystallite size, λ indicates the wavelength, β denotes the peak lines, k represents the shape factor, θ is the Bragg's diffraction angle [14]. The average crystallite size of α-Fe_2O_3 nanoparticles was calculated using Scherrer's formula and found to be 45.1 nm.

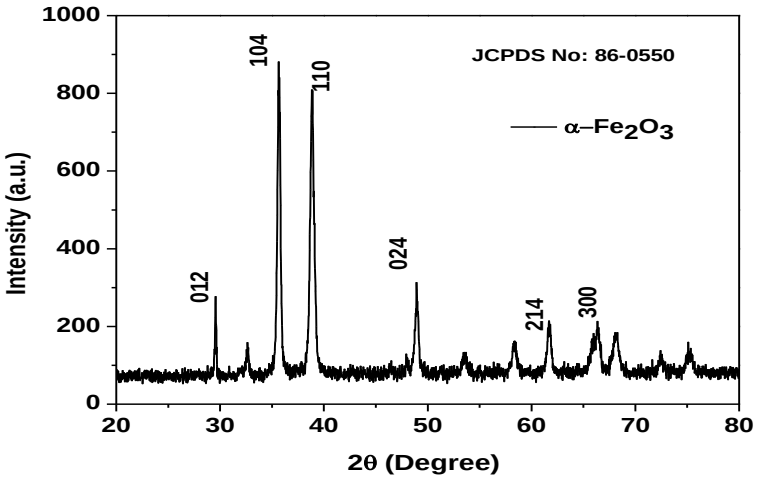

Figure 1: Fabrication of iron oxide nanoparticles in XRD pattern

3.2. FT-IR analysis of Fe_2O_3 NPs

FT-IR analysis was used to identify functional groups present in the range of 400 to 4000 cm^{-1}. The α-Fe_2O_3 NPs FT-IR results are given in Figure 2. The stretching mode of aromatic O–H is visible at 3392cm^{-1}[15]. The other characteristics peaks of CH_3 and CH_2 are visible at 2935cm^{-1} and 1639cm^{-1}, respectively. C–H overtones resulted in a peak at 1428cm^{-1}. Spectra of aromatic rings C=C show the stretching mode at a wavelength of 1161 cm^{-1}, Although methylene C-H bending mode occurs between 1032cm^{-1}. The peak at 843 cm^{-1} is the result of M-O-M bending. The peak at 569 cm^{-1} is occurred due to the stretching vibrations of iron oxide. The reduction of metals and the capping of iron oxide nanoparticles were accomplished by the phytochemicals available in the seed extract. The iron oxide nanoparticles formation has been confirmed by FT-IR analysis [15].

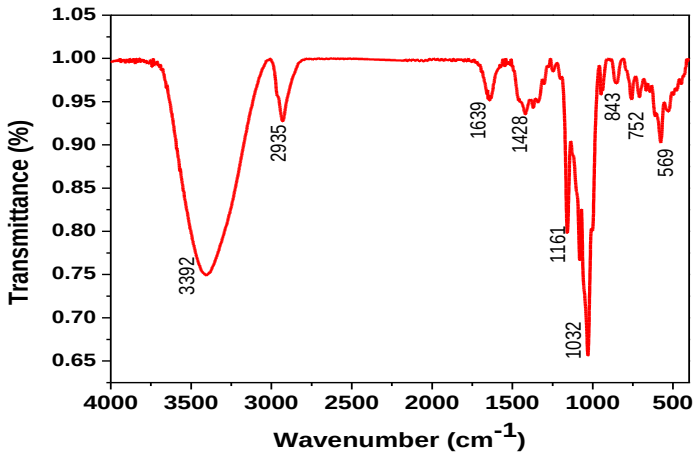

Figure 2: The FT-IR spectra of iron oxide nanoparticles

3.3. SEM analysis with EDX of Fe_2O_3 NPs

Figure 3(a) shows the morphology of synthesised iron oxide nanoparticles by SEM analysis. The SEM image shows that iron oxide nanoparticles were formed in spherical shape. The results also show that particles are agglomerated in nature. The presence of stabilizing, reducing and capping agents in lotus seed extract may promote the formation of nanoparticles with less agglomeration and spherical in shape. The energy dispersive X-ray (EDX) analysis was conducted to determine the elemental composition of prepared samples, as shown in Figure 3(b). The EDX spectrum indicates that the prepared sample consists of Fe (90.11%) and O (9.89%) only. The distribution of Fe and oxygen O confirms the homogeneity of the sample. Histogram distribution plot from SEM image shown in Figure 3(c), demonstrated that the average size of was found to be 45.1 nm using Image J software.

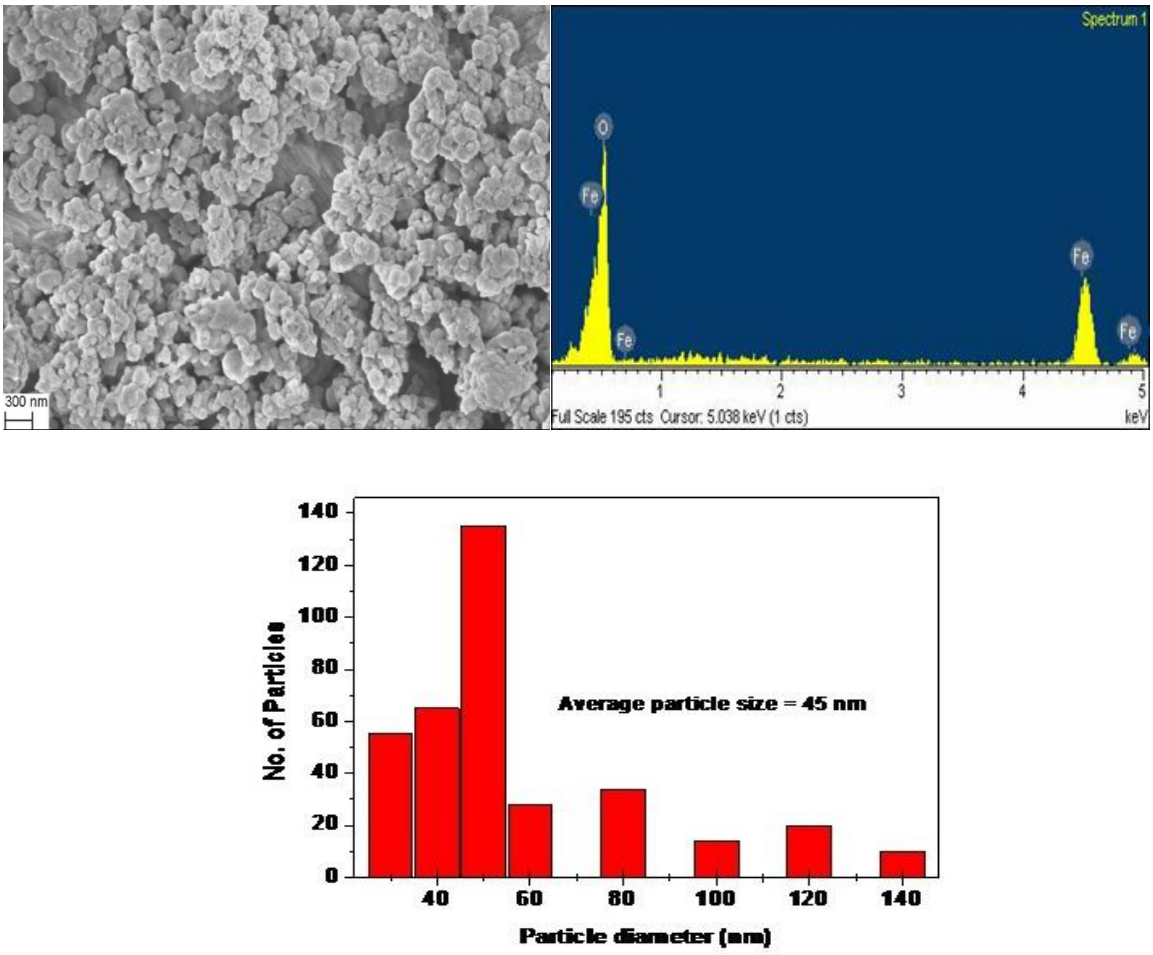

Figure 3 (a): SEM analysis and (b): EDX spectrum of iron oxide nanoparticles (c): histogram of the particle size distribution of α-Fe_2O_3 NPs from SEM analysis

3.4. UV– visible spectroscopy

The UV–Visible absorption spectra of α-Fe_2O_3 NPs synthesized using green methods were analysed at room temperature. Figure 4 shows the UV–Visible spectroscopy results of α-Fe_2O_3. The results indicate that it has strong light absorption ability. Also it suggests that the there was a quick movement of electrons from the valence band to the conduction band energy was occurred [16]. The band gap of iron oxide nanoparticles was determined using the equation $E = hc/\lambda$, where h is Planck's constant, c is the speed of light, and λ is the wavelength. The UV–Visible spectrum of lotus seeds extract showed a peak at 452 nm, indicating the stability of the formed iron oxide nanoparticles, with the higher intensity suggesting a high yield

of nanoparticles. The bandgap energy of 2.74 eV was calculated and is consistent with the band gap values reported in the literature [16].

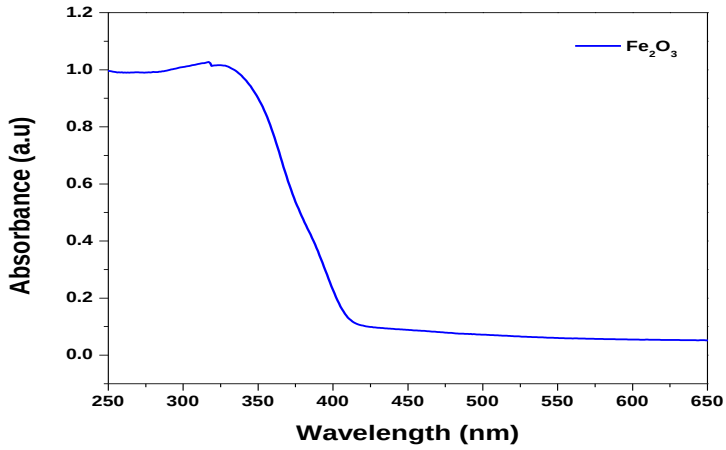

Figure 4: UV – Visible spectrum of iron oxide nanoparticles

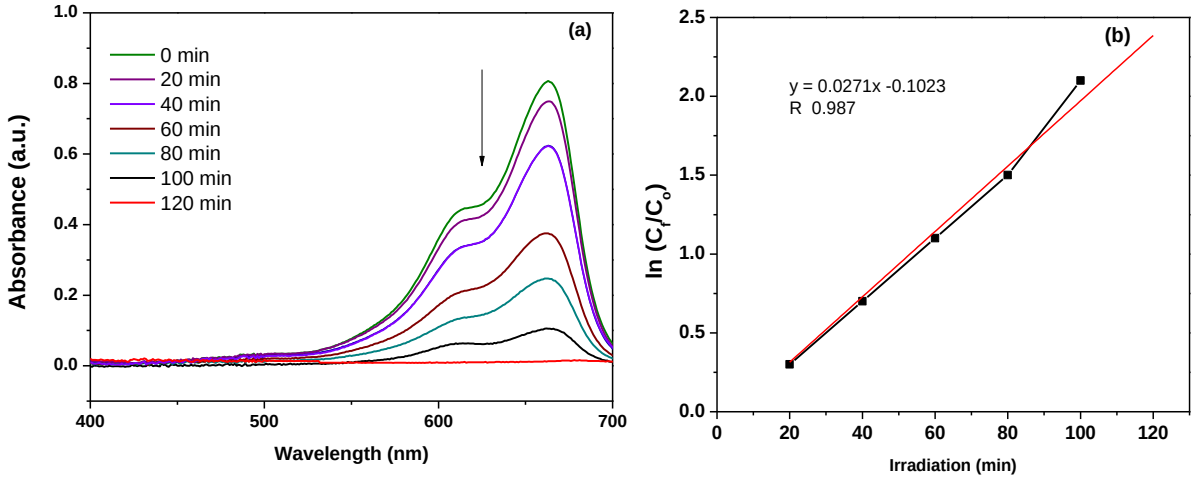

Figure 5(a): Photocatalytic absorbance spectrum of iron oxide nanoparticles, (b): Plot of ln (C_f/C_o) as a function of irradiation time for MO dye

3.5. Photocatalytic activity

The photocatalytic activity of α-Fe_2O_3 NPs for MO degradation was studied under visible light using a 250 W Halogen lamp. Figure 5(a) shows the reduction of absorption peaks of MO dye during the photodegradation reaction. In 50 ml of methyl orange solution, 10 mg of catalyst (α-Fe_2O_3 NPs) was added. The solution was stirred for one hour in a dark environment to attain adsorption – desorption equilibrium, the degradation test was carried out to determine the photocatalytic behaviour of biosynthesis mediated iron oxide nanoparticles. The kinetics study for photocatalyst of MO dye by iron oxide sample is represented in Figure 5(b). The decreased dye absorption peak over time suggests that complete breakdown of dye molecules into smaller organic acids. The solution was examined using UV–Visible spectrometer to determine the concentration of dye compounds after degradation process at regular time intervals. The dye degradation efficiency was calculated using the equation, Degradation efficiency (%) = [$C_i - C_f$ / C_i]× *100*. In this equation, C_i refers initial absorbance of the dye solution; C_f denotes absorbance after photocatalytic activity [17]. The significant photodegradation activity exhibited by the biosynthesised α-Fe_2O_3 NPs nanoparticles is compared with previous reports as shown in Table.1. The higher MO degradation efficiency can be attributed to the higher activity of α-Fe_2O_3 nanoparticles prepared using

biosynthesis route. The hydroxyl radicals generated during the photoreactions promotes the redox reactions to degrade the MO dye molecules. In particular, α-Fe_2O_3 prepared through biosynthesis approach efficiently captures the electrons and remarkably decreased the electron-hole pair recombination events [18-20]. The mechanism depends on the generation of superoxide radicals ($\bullet O_2^-$) and hydroxyl radicals (•OH). The radical species play a crucial role in the degradation process to attack the Methyl Orange (MO) dye molecules in order to break their complex structure into simple and smaller molecules [21-24].

Table 1 Comparison of various dye degradation of Fe_2O_3 NPs

Dye	Type of Catalyst	Excitation wavelength (nm)	Catalyst Amount (mg)	Volume of dye Solution (ml)	Degradation Efficiency (%)	Time (min)	Preparation method	Reference
Rh B	Husked rice-shaped iron oxide nanoparticles (Fe_2O_3 NPs)	393	50	50	92%	50	Biogenic Preparation	[16]
MB	Hematite α-Fe_2O_3 NPs from iron chloride ($FeCl_2{\cdot}2H_2O$) solution using Mentha pulegium extract	256 to 300	10	100	78.68%	120	Biosynthesis	[17]
MO	Ferric chloride ($FeCl_3{\cdot}6H_2O$)	465 to 490	10	8	77%	360	Plant extract method	[18]
MO	$FeNbO_4$ monoclinic nanocomposite	365 to 395	15	20	96%	50	Hydrothermal and sol gel methods	[19]
MB	Ag/CuO and Ag/TiO_2	380	10	40	86%	40	Chemical-free and plasmon-driven Synthesis	[20]
MO	Iron Oxide Nanoparticles using Lotus Seeds	452	10	50	93.5%	120	Green Synthesis	**Present work**

CONCLUSION

α-Fe_2O_3 NPs were successfully prepared through green synthesis approach using lotus seed extract. SEM and XRD analysis confirmed that the iron oxide nanoparticles were obtained with high crystallinity and lesser agglomeration. This result suggests that recombination centers for photogenerated charge carriers and lower unoccupied molecular orbital were generated while using the biomediated preparation route. FT-IR results suggest the successful fabrication of all α-Fe_2O_3 NPs. The reduction in band gap is due to the green synthesis route that generates additional electronic states which facilitated to attain decreased band gap and enhanced light-absorption characteristics, which would lead to achieve increased photocatalytic degradation rate. Higher photodegradation efficiency (93.5 % in 120 min) of MO was obtained in this work which was compared with other reports. The improved degradation rate of MO dye could be attributed to the fast charge transfer, reduced band gap and a decreased electron-hole pair recombination rate. The results of this work could offer a low-cost, less energy and green synthesis route to extend the photoactivity into visible range and also for scaled-up operations to treat various other dyes.

REFERENCES

[1] Abdullah, Tahir Hussain, Shan Faisal, Muhammad Rizwan, Saira, Nasib Zaman,Madiha Iqbal, Arshad Iqbal, Zafar Ali, 2022. Green synthesis and characterization of coper and nickel

hybrid nanomaterials: Investigation of their removal of organic crystal violet dye, Journal of Saudi Chemical Society 26, 101486.

[2] Tola Jabessa Masho, Ponnusamy ThillaiArasu, Raji Feyisa Bogale, Kemal Mohammed Gendo, 2024. Green synthesis, characterization of Ag_2O doped ZnO nanoparticles using aqueous extract of Croton macrostachyus leaf for photo degradation, and antioxidant activities, Result in Chemistry 7, 101478.

[3] KhaoulaHkiri, Hamza Elsayed, Ahmed Mohamad, Naomi Harrisankar, Alain Gibaud, Eric Van Steen, MalimMaaza, 2024. Environmental water treatment with green synthesized WO_3 nanoflakes for cationic and anionic dyes removal: Photocatalytic studies, Catalysis Communications 187, 106851.

[4] Veronica Rocha, Sandra Franco, Ana Raquel Bertao, Isabel C. Neves, Teresa Tavers, 2024. Recycling of natural and waste materials as supports for green sliver nanoparticles as efficient catalyst in photodegradation of organic pollutants, Environmental Technology & Innovation 34, 103576.

[5] Pradnya V. Patil, Nisha A, Nerlekar, Aviraj R. Kuldeep, Pradnya P. Patil, Prafull B. Dandge, Turkaram D. Dongale, Padma B. Dandge, Gajanan S. Rashinkar, 2024. Terminalia bellirica (Gaertn.) Roxb.extract – mediated green synthesis of magnesium oxide nanoparticles for multifunctional application, Plant Nano Biology 8, 100069.

[6] Haewon Byeon, Hitendra Kumar Lautre, N.R. Rajagopalan, M. Sivaprakash, Giriraj Kiradoo, Adisu Haile, R.A. Arul Raja, J. Sunil,2024. Facile preparation of Fe_2O_3 catalyst and assessment of its photodegradation performance for industrial effluent purification, Results in Chemistry, 7, 101435.

[7] Nanda Saridewi, DiendaJuitaUtami, AgustinoZulys, Siti Nurbayti, NurhasniAdawiah, AngginaRahma Putri, Rumi Kamal, 2024. Utilization of Lidahmeruta (Sansevieriatrifasciata) extract or green synthesis of $ZnFe_2O_4$ nanoparticle as visible-light responsive photocatalyst for dye degradation, Case Studies in Chemical and Environmental Engineering 9, 100745.

[8] Zakie Aalami, Mohammad saleh Hoseinzadeh. Parsa Hosseini Manesh, Amir Hossein Aalami, Zarrin Es haghi. MakidDarroudi, Amirhossein Sahebkar, Hasan Ali Hosseini, 2024. Synthesis, characterization, and photocatalytic activities of green sol-gel ZnO nanoparticles using Abelmoschus esculentus and salvia officinalis: A comparative study versus co-precipitation-synthesized nanoparticles, Heliyon 10, E24212.

[9] Amir Azizi, Marziyeh Kazemi, 2024. Green synthesis of zinc oxide magnetic nanocomposite via zinc electroplating effluent: Its characterization and application and application as a photocatalyst, Result in Optics 16, 100698.

[10] Jeevan Mathew Tharayil, Prakash Chinnaiyan, 2023. Biogenic synthesis of ZnO from Rubiacordifolia root extract: A study on sono-photocatalytic dye degradation and anti-bacterial assay, Result in Engineering 20, 101567.

[11] Sammy Indire Wanakai, Patrick GachoKiKareru, David Sujee Makhanu, Edwin Shigwenya Madivoli,2022. Advances in green nanotechnology: Data for green synthesis and characterization of iron nanoparticles synthesized using Galinsoga Parviflora, Conyzabonariensis and Bidens Pilosa leaf extracts, and their application in degradation of methylene blue dye and rifampicin antibiotic, Data in Brief 46, 108882.

[12] Saba Ameen, Zaib Hussain, Muhammad Imran Din, Rafi Ullah Khan, Rida Khalid, 2024. Green Synthesis of Biochar@Al2O3 Nanocomposite from Waste Melia Azedarach Fruit Biomass Pyrolysis: A Sustainable Solution for Photocatalytic Methylene Blue Dye Degradation, Desalination and Water Treatment 320, 100609.

[13] Geetha Malini Palani Singaram, Rani Selvaraj, 2024. Photocatalytic degradation of acid violet dye by sun light exposure using green synthesized magnesium oxide nanoparticles, Chemical Physics Impact 8, 100628.

[14] Shazia Nouren, Ismat Bibi, AbidaKausar, Misbah Sultan, Haq Nawaz Bhatti, Yusra Safa, Sana Sadaf, NoragAlwadi, Munawar Iqbal, 2024. Green synthesis of CuO nanoparticles using Jasmin Sambac

extract: conditions optimization and photocatalytic degradation of Methylene Blue dye, Journal of King Saud University – Science 36, 103089.

[15] Vinay Viswanath Konduri, Naveen Kumar Kalagatur, Lokanadhan Gunti, Usha Kiranmayi Mangamuri, Venkateswara Rao Kalagadda, Sudhakar Poda, Suresh Babu Naidu Krishna, 2024. Green synthesis of silver nanoparticles from Hibiscus tiliaceus L. Leaves and their application in dye degradation, antioxidant, antimicrobial, and anticancer activities, South African Journal of Botany 168, 476–487.

[16] Abinaya Rajendran, Murad Alsawalha, Thamer Alomayri, 2021. Biogenic synthesis of husked rice-shaped iron oxide nanoparticles using coconut pulp (Cocos nucifera L.) extract for photocatalytic degradation of Rhodamine B dye and their in vitro antibacterial and anticancer activity, Journal of Saudi Chemical Society 25, 101307.

[17] Mohamed Bilal Goudjil, Halima Dali, SouadZighmi, Zineb Mahcene, Salah EddineBencheikh, 2024. Photocatalytic degradation of methylene blue dye with biosynthesized Hematite α-Fe_2o_3 nanoparticles under UV-Irradiation, Desalination and Water Treatment 317, 100079.

[18] Lelli Shaker Ardakani, Vahid Alimardani, Ali Mohammed Tamaddon, Ali Mohammad Amani, Saeed Taghizadeh, 2020. Green synthesis of iron-based nanoparticles using chlorophytum comosum leaf extract: methyl orange dye degradation and antimicrobial properties, Heliyon 7, E06159.

[19] Bayahia, H. 2024. Schinus mole extract mediated green synthesis of iron niobite photocatalyst for the degradation of methyl orange dye under visible light, Journal of Saudi Chemical Society 28, 101876.

[20] Helen Rathi, V., Ambrose Rejo Jeice, Kumarasamy Jayakumar, 2023. Green synthesis of Ag/CuO and AG/TIO_2 nanoparticles for enhanced photocatalytic dye degradation, antibacterial, and antifungal properties, Applied Surface Science Advances 18, 100476.

[21] Gomathy, M., Deepa, M., Vanitha Arumugam, Rekha Pachaiappan, Padmavathi Rajangam, 2024. An effective antimicrobial effect by silver doped zinc oxide nanoparticles prepared by co-precipitation method. Int. J. Adv. Sci. Eng.,10, 3734-3744.

[22] Yasotha, P., Kalaiselvi, V., Vidhya, N., Ramya, V.2020. Green Synthesis and Characterization of Zinc Oxide Nanoparticles using Ocimum Tenuiflorum. Int. J. Adv. Sci. Eng., 7, 1584-1588.

[23] Aklilu Guale Bekru, Lemma Teshome Tufa, Osman Ahmed Zelekew, Mahendra Goddati,Jaebeom Lee, Fedlu Kedir, Sabir. 2022. Green Synthesis of a CuO–ZnO Nanocomposite for Efficient Photodegradation of Methylene Blue and Reduction of 4-Nitrophenol. American Chemical Society. 7 (35)30908–30919.

[24] Hildana Tesfaye Berede, Dinsefa Mensur Andoshe, Noto Susanto Gultom, Dong-Hau Kuo, Xiaoyun Chen, Hairus Abdullah, Tadele Hunde Wondimu, Yi-nan Wu, Osman Ahmed Zelekew.2024. Photocatalytic activity of the biogenic mediated green synthesized CuO nanoparticles confined into MgAl LDH matrix. Scientific reports.14, 2314